Contents lists available at ScienceDirect

Agricultural Water Management

journal homepage: www.elsevier.com

A geo-informatics approach for estimating water resources management components and their interrelationships

Umar Waqas Liaqat [a, b], Usman Khalid Awan [c], Matthew Francis McCabe [b], Minha Choi [d, *]

[a] Department of Civil and Environmental Engineering, College of Engineering, Hanyang University, Seoul 133-791, Republic of Korea
[b] Water Desalination and Reuse Center, Division of Biological and Environmental Sciences and Engineering, King Abdullah University of Science and Technology, Thuwal, Saudi Arabia
[c] International Center for Agricultural Research in the Dry Areas (ICARDA), 15 Khalid Abu Dalbouh St., Abdoon EShamali, P.O. Box, Amman, 950764, Jordan
[d] Water Resources and Remote Sensing Laboratory, Department of Water Resources, Graduate School of Water Resources, Sungkyunkwan University, Suwon 440-746, Republic of Korea

ARTICLE INFO

Article history:
Received 14 September 2015
Received in revised form 15 July 2016
Accepted 14 September 2016
Available online xxx

Keywords:
SEBS
Water scarcity
Groundwater abstraction
Groundwater recharge
Remote sensing
GIS

ABSTRACT

A remote sensing based geo-informatics approach was developed to estimate water resources management (WRM) components across a large irrigation scheme in the Indus Basin of Pakistan. The approach provides a generalized framework for estimating a range of key water management variables and provides a management tool for the sustainable operation of similar schemes globally. A focus on the use of satellite data allowed for the quantification of relationships across a range of spatial and temporal scales. Variables including actual and crop evapotranspiration, net and gross irrigation, net and gross groundwater use, groundwater recharge, net groundwater recharge, were estimated and then their interrelationships explored across the Hakra Canal command area. Spatially distributed remotely sensed estimates of actual evapotranspiration (ET_a) rates were determined using the Surface Energy Balance System (SEBS) model and evaluated against ground-based evaporation calculated from the advection-aridity method. Analysis of ET_a simulations across two cropping season, referred to as *Kharif* and *Rabi*, yielded Pearson correlation (R) values of 0.69 and 0.84, Nash-Sutcliffe criterion (NSE) of 0.28 and 0.63, percentage bias of −3.85% and 10.6% and root mean squared error (RMSE) of 10.6 mm and 12.21 mm for each season, respectively. For the period of study between 2008 and 2014, it was estimated that an average of 0.63 mm day^{-1} water was supplied through canal irrigation against a crop water demand of 3.81 mm day^{-1}. Approximately 1.86 mm day^{-1} groundwater abstraction was estimated in the region, which contributed to fulfil the gap between crop water demand and canal water supply. Importantly, the combined canal, groundwater and rainfall sources of water only met 70% of the crop water requirements. As such, the difference between recharge and discharge showed that groundwater depletion was around −115 mm $year^{-1}$ during the six year study period. Analysis indicated that monthly changes in ET_a were strongly correlated (R = 0.94) with groundwater abstraction and rainfall, with the strength of this relationship significantly ($p < 0.01$ and 0.05) impacted by cropping seasons and land use practices. Similarly, the net groundwater recharge showed a good positive correlation (R) of 0.72 with rainfall during *Kharif*, and a correlation of 0.75 with canal irrigation during *Rabi*, at a significance level of $p < 0.01$. Overall, the results provide insight into the interrelationships between key WRM components and the variation of these through time, offering information to improve the management and strategic planning of available water resources in this region.

1. Introduction

Agriculture is one of the mainstays of Pakistan's economy, contributing more than 25% to the nation's GDP and employing almost half of the adult population (Bhatti et al., 2009; Yu et al., 2013). The sustainability of agriculture is almost wholly dependent on irrigation water supplies, provided via one of the world's largest irrigation networks. However, despite considerable capital expenditure on the maintenance and operation of this system, it is ranked as one of the most mismanaged irrigation systems in the world (Yu et al., 2013). Mismanagement has contributed to a range of problems including land and environmental degradation, waterlogging and salinity, inequitable distribution of water, and social and institutional conflicts (Laghari et al., 2012). Sustained increases in population growth coupled with competing agricultural water users across the Indus Basin of Pakistan dictates the need to implement improved water management practices in the region (Ahmad et al., 2009; Kirby et al., 2016).

Clearly, the strategic management of available water resources is of paramount importance in understanding and predicting the hydrological behavior of this complex system (Awan et al., 2016; Cheema et al., 2014). To do this requires the identification and estimation of strategic water resources management (WRM) components across both time and space domains. Such detailed monitoring of WRM components can be used as a screening tool towards sustainable use of basin scale water resources (Hertzog et al., 2014) in an optimal way for socio-economic development. This can be achieved by implementing a geo-informatics approach, which integrates key remote sensing derived hydrological variables, auxiliary ground measure-

* Corresponding author at: Department of Water Resources, Graduate School of Water Resources, Sungkyunkwan University, 2066 Seobu-ro, Jangan-gu, Suwon Gyeonggi-do, 440-746, Republic of Korea.
Email addresses: umar.liaqat@kaust.edu.sa (U.W. Liaqat); mhchoi@skku.edu, minha1218@gmail.com (M. Choi)

http://dx.doi.org/10.1016/j.agwat.2016.09.010
0378-3774/

ments and geo-statistics as an information source to a Geographic Information System (GIS) for analytical assessment. A combined data modelling and geo-informatics approach provides an intelligent spatial hydrological analysis that helps in describing the variation and uncertainties in WRM components associated with atmospheric, surface and sub-surface water fluxes (Ahmad et al., 2005).

The lack of spatio-temporal observation data in many arid and semi-arid environments hampers the quantification of WRM components (Becker, 2006; Brunner et al., 2007). One means to address the lack of spatially distributed information is through the use of satellite remote sensing techniques, which can provide spatially continuous datasets of a number of variables (Boegh et al., 2009; Campos et al., 2013; Milewski et al., 2009). For instance, there is an extensive history of using remote sensing data for the estimation of hydrological components such as evapotranspiration (ET) (Ershadi et al., 2014; Liaqat and Choi, 2015; McCabe et al., 2005), which serves as a critical variable in the characterization of groundwater systems (Becker, 2006).

Groundwater is considered as a prime water resource in arid and semi-arid regions with the potential to bridge the gap between crop evapotranspiration (ET_c) and effective rainfall or surface water supplies (Chowdary et al., 2008; Mastrocicco et al., 2010). Declining, or even stable surface irrigation water availability, is putting greater pressure on farmers to supplement water supplies with groundwater in order to meet the needs of growing populations and increasing food demands (De Vries and Simmers, 2002). Such adjustments have resulted in dramatic drops in regional groundwater tables by approximately 1–3 m $year^{-1}$, as observed in various geographical settings of South and East Asia (Kinzelbach et al., 2003; Kirby et al., 2015; Yang et al., 2015). Groundwater abstraction in the irrigated Indus Basin of Pakistan range between 30 and 60% of total crop water requirements (Sarwar and Eggers, 2006; Scott and Shah, 2004), largely as a consequence of an unreliable water supply from surface irrigation (Cheema et al., 2014). For these reasons, the reliable quantification of net and gross groundwater use in space and time is critically important to develop sound groundwater management policy for sustainable exploitation.

Net groundwater recharge represents one of the most challenging components of WRM due to difficulties with its direct measurement (Anuraga et al., 2006; Castaño et al., 2010; Crosbie et al., 2015). Several approaches exist to quantify groundwater recharge, all with their own advantages and limitations (Scanlon et al., 2002). The conceptually simple water balance approach has gained considerable attention due to its simplicity and reliable estimation by use of remote sensing observations (Szilagyi et al., 2011). A number of previous studies have used this method for the determination of spatio-temporal groundwater recharge in the United States, Europe and Africa (Huang et al., 2013; Műnch et al., 2013; Szilagyi and Jozsa, 2013; Szilágyi et al., 2012) by only considering the difference in precipitation and ET. Such studies tend to ignore changes in soil moisture and surface irrigation supplies, which could lead to significant errors in net groundwater recharge estimation due to extreme variability in irrigation contributions from rivers or canals. Errors and variability associated with remotely sensed ET in heterogeneous environments with poor spatial density of needed meteorological measurements also presents as a potential source of uncertainty (Ershadi et al., 2013a; Liou and Kar, 2014).

The present study focuses on the estimation of various WRM components, as well as their interrelationships, over the Hakra Canal command area in eastern Pakistan during the period of April 2008 to March 2014. The specific components that are estimated include the actual evapotranspiration (ET_a), crop evapotranspiration (ET_c), net and gross irrigation, net and gross ground water use, recharge, net recharge, and rainfall. In addition to quantifying their spatial and temporal behavior, identifying correlation between WRM components allows for an analysis of the impact of intervention strategies on these statistical relationships to be determined. Furthermore, improved knowledge of these interrelationships will provide a mechanism through which plausible ranges of water resources allocations within the irrigation scheme can be determined and assessed (Awan et al., 2013; Cheema et al., 2014).

2. Study area

The Hakra canal command encompasses an area of approximately 0.2 Mha and has an arid to semi-arid climate that is representative of a typical irrigation area of the Indus basin. The region is situated in the southeast of the Punjab province of Pakistan (Fig. 1) with its mapping extent between latitude 29.05° to 29.95° north and longitude 72.26° to 73.40° east. Surface topography in the irrigation scheme gradually decreases from 176 m above mean sea level in the upper north of the basin to less than 125 m above mean sea level towards south-west (Shafeeque et al., 2016). The Hakra irrigation scheme is comprised of 17 major irrigation distributaries that historically delivered water through several minor canals and direct water courses (Fig. 1a). The groundwater table in the study region ranges between 1 and 25 m (Shafeeque et al., 2016), while depth to groundwater (DTGW) is being monitored on a seasonal basis through eleven distributed observation wells, as depicted in Fig. 1a. Rainfall is insufficient to meet the crop water requirements of the region, which forces farmers to use canal water, ground water or a combination of both to support their consumptive needs. However, even with these additional sources, it is generally insufficient to meet the crop water requirements.

There are several social and institutional conflicts on access to canal water, as it is much cheaper when compared with groundwater extraction. To resolve these issues and to determine an equitable distribution of canal water, the irrigation system is being managed via public-private partnerships. Although, farmer representatives are involved in the local irrigation scheme, with an aim to achieve equity and to improve cost recovery, the equitable management of irrigation waters remains challenging (Awan et al., 2016). Erratic surface water deliveries enhances (and encourages) the use of pumped groundwater to achieve a certain agriculture production level.

The study area is broadly classified as agricultural land, and has a number of major crops including rice, cotton, fodder, millet, gram, rapeseed and wheat, which are grown in rotation, depending upon the cropping season (see Fig. 1b). The area has two main cropping seasons, defined as *Kharif* (April-September) and *Rabi* (October-March). A land use land cover (LULC) classification map of the study region (Fig. 1b) was developed at a spatial resolution of 250 m by using the Normalized Difference Vegetation Index (NDVI), available from the Moderate Resolution Imaging Spectroradiometer (MODIS) and following the methodology of Awan and Ismaeel (2014). Wheat is the main crop cultivated during *Rabi*, while rice and cotton are the major crops during *Kharif*. There is a strong seasonality in both temperature and rainfall (see Fig. 2), with maximum rainfall occurring during the monsoon period from June to September, which accounts for about 50% of the average annual rainfall of 318 mm $year^{-1}$ over the study period. More than 80% of the total rainfall occurs during *Kharif*, while *Rabi* receives the remaining 20%. Daytime minimum and maximum temperature ranges between 20 °C and 43 °C in *Kharif,* and between 6 °C and 25 °C during *Rabi* season (Fig. 2).

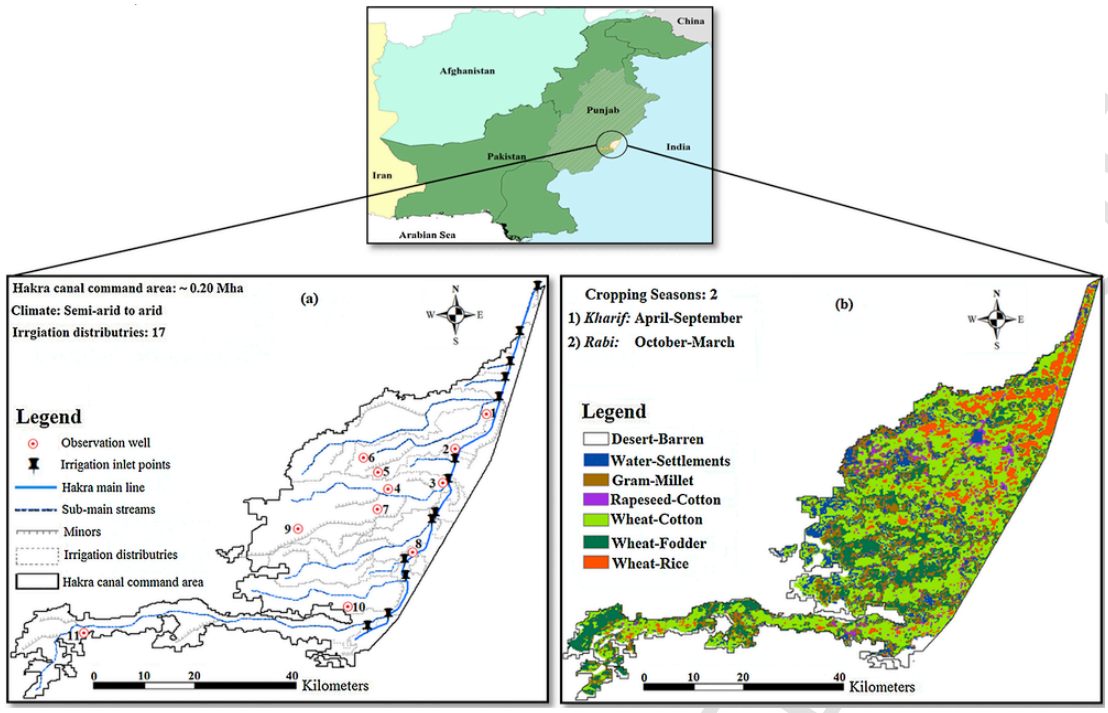

Fig. 1. Geographical location of the Hakra canal command area including (a) the position of irrigation distributaries, observation wells and (b) land use classification map.

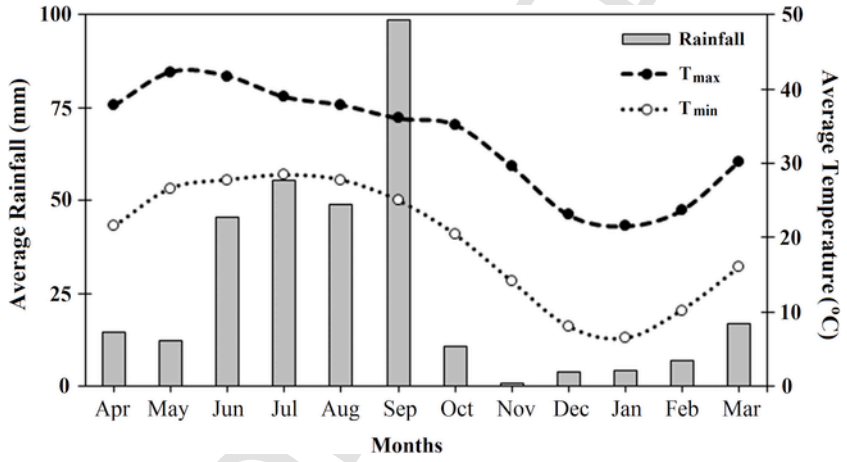

Fig. 2. Average monthly variation of rainfall, and maximum and minimum temperatures during the study period (2008–2014) in the Hakra canal command area.

3. Water resources management (WRM) components and their correlation

Nine WRM components were identified for operational and strategic planning of water resources in the Hakra canal command area. As noted earlier, these include actual and crop evapotranspiration, net and gross canal water use, net and gross groundwater use, groundwater recharge, net groundwater recharge, and rainfall. Fig. 3 illustrates the framework that was used to estimate these components during the period from April 2008 to March 2014. Pixel by pixel based actual evapotranspiration (ET_a) was determined using the Surface Energy Balance System (SEBS; Su, 2002) model, which has been extensively evaluated in the literature (Byun et al., 2014; Ershadi et al., 2014; Su et al., 2005). Net groundwater use is quantified by incorporating satellite driven ET_a rates within a geo-informatics approach, without the need for often complex ground water models. Such an approach, with its higher accuracy, computational efficiency and minimal need for field data, has advantages over more conventional direct and indirect methods (Ahmad et al., 2005) and has been successfully implemented in different regions around the world (Ahmad et al., 2005; Campos et al., 2013; Castaño et al., 2010). The losses at farm and network level were incorporated to estimate gross groundwater abstraction, while groundwater recharge was determined by estimating the fraction (0.9) of difference between gross and net irrigation amount that recharge the aquifer. Net groundwater recharge at a spatial resolution of 1-km was derived by subtracting discharge from recharge values. After reliable quantification, a correlation between all components was determined on seasonal and annual basis to ex-

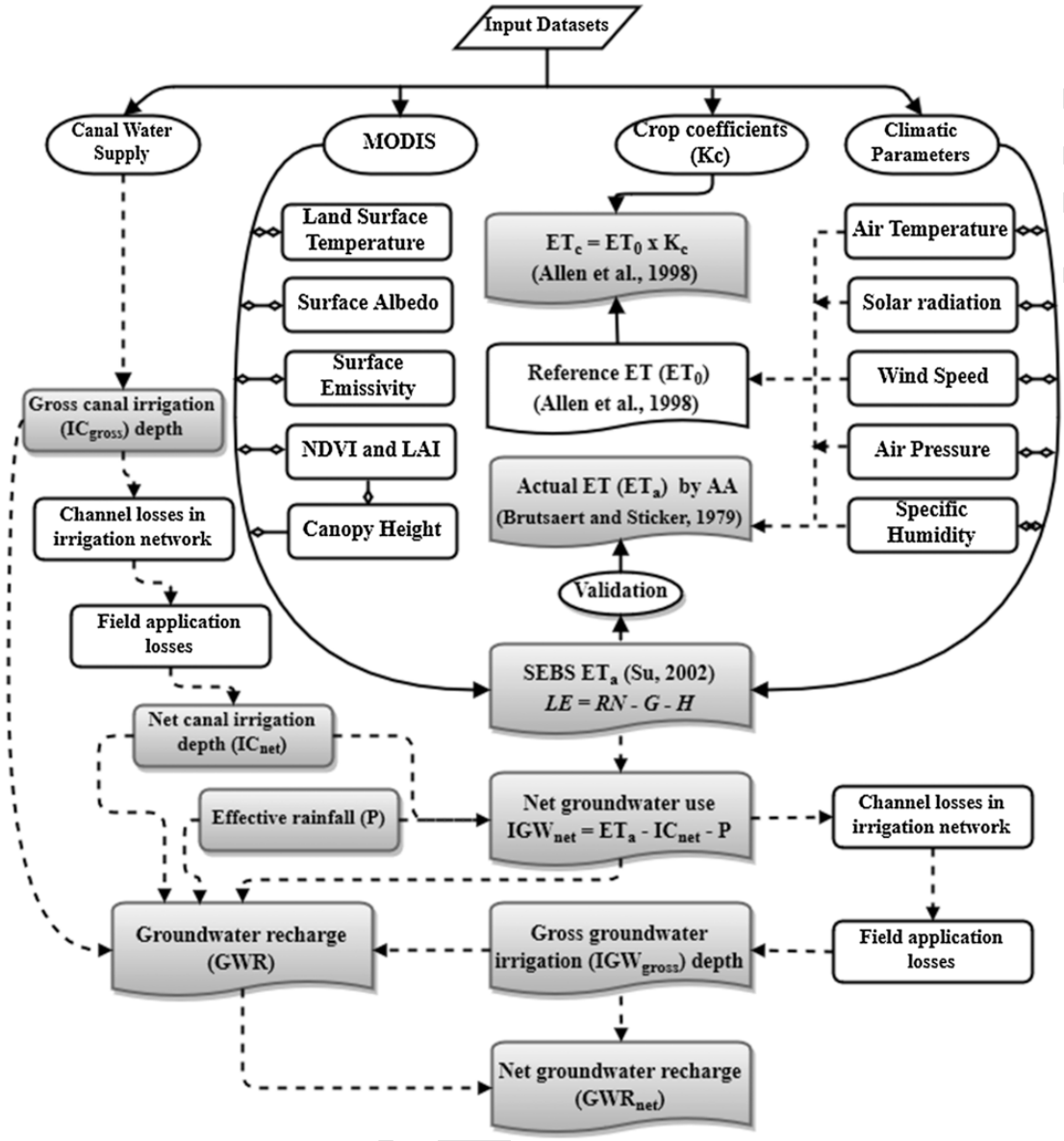

Fig. 3. A flowchart summary explained methodological framework (n.b.: gray filled boxes show final outputs).

amine the impact of input irrigation water resources on outgoing fluxes.

3.1. Actual evapotranspiration

The SEBS model (Su, 2002) uses a combination of in-situ meteorological, ancillary data and remote sensing information to determine the terrestrial heat fluxes. After calculating the sensible heat flux via use of the Monin-Obukhov similarity theory (Byun et al., 2014; McCabe et al., 2005), the ET_a is determined as a residual of the surface energy balance equation. The main inputs to this algorithm is a combination of visible, near-infrared and thermal infrared satellite data, together with ground based meteorological data. A detailed description of the algorithm is presented in several previous studies where this model is validated under diverse ago-climatic conditions (Ershadi et al., 2014; Liaqat and Choi, 2015). A number of related studies have shown that SEBS can estimate ET_a at a range of spatio-temporal scales and can provide an error of less than 15%, if parameterized correctly (Ershadi et al., 2013b; Su et al., 2005).

The model is based on solving the surface energy budget, with ET_a as a residual product as given below:

$$\lambda E = R_N - G - H \tag{1}$$

where R_N = net radiation (W m^{-2}); G = soil heat flux (W m^{-2}); H = sensible heat flux (W m^{-2}); and λE = latent heat flux (W m^{-2}). After solving for a set of complex equations describing stability functions for momentum and heat transfer (Liaqat et al., 2015; Su, 2002), evaporative fraction (EF), which expresses the ratio of actual evaporation to the total available energy, can be determined as follows:

$$EF = \frac{\lambda E}{R_N - G} \tag{2}$$

The EF calculated at the satellite overpass time is often assumed to remain relatively constant across the diurnal cycle (Cragoa and Brutsaert, 1996; Sugita and Brutsaert, 1991) and can therefore be used to extrapolate instantaneous ET_a to daily timescales, after estimating the net available energy. The daily ET_a values can then be aggregated to monthly and seasonal scale (Liaqat et al., 2015). The use of a daily net available energy is important when considering the difference in ET_a from clear to all sky conditions. For timescales of one day, the daily actual evapotranspiration (ET_{daily}) is calculated as follows:

$$ET_{daily} = 8.64 \times 10^7 \times EF \times \frac{R_{N24} - G_{24}}{\lambda \rho_w} \quad (3)$$

where R_{N24} = 24 h averaged net radiation, G_{24} is the daily soil heat flux (which is assumed to be zero at the daily scale following Allen et al., 1998), λ = latent heat of vaporization (2.47×10^6 J kg^{-1}), and ρ_w = density of water (kg m^{-3}).

3.1.1. Satellite and meteorological forcing data

MODIS Level 3 atmospherically corrected data products were used to estimate evapotranspiration from the SEBS algorithm, due to their optimal spectral bands, high temporal resolution and availability over the study region. A total of 720 clear sky images (defined as having less than 10% cloud cover within the scene) of land surface temperature and emissivity (MOD11A1) were downloaded from the MODIS data distribution website (https://lpdaac.usgs.gov/get_data/data_pool). Table 1 details a list of related data products that were used in the calculation of ET_a, including surface albedo (MCD43B3), leaf area index (LAI) (MOD15A2) and normalized difference vegetation index (NDVI) (MOD13A2). SEBS uses NDVI to develop canopy height maps, which is an important variable used in the estimation of aerodynamic resistance (Liaqat et al., 2015).

In addition to MODIS image products, routine climatic parameters required to implement SEBS were collected from Bahawal Nagar meteorological station maintained and operated by the Pakistan Meteorological Department (PMD). Rainfall on a monthly basis from 2008 to 2014, as well as data on min and max temperature, wind speed, solar radiation, surface pressure and relative humidity, were collated from the archives of the PMD. The effective rainfall, determined as 80% of the total rainfall amount for this arid region (Adnan and Khan, 2009), was used to derive key WRM components, as described below in Section 3.7.

3.1.2. Evaluation of SEBS retrievals

The accuracy of SEBS-retrieved ET_a is important in the reliable determination of other water balance components and for establishing meaningful statistical relationships between them. In many cases, results derived from remote sensing based evaporation models are usually compared with point measurements of ET_a collected from eddy covariance based flux towers (Choi et al., 2009, 2011), soil water balance methods (Santos et al., 2008), Bowen ratio energy balance approaches (Singh and Irmak, 2011) or from a weighing lysimeter (Gowda et al., 2013). Since in-situ based instrumentation were not available for the study area, the SEBS model performance was assessed against ground based ET_a calculated from an advection-aridity (AA) method (Liaqat et al., 2015).

The AA method can be formulated by combining information from the energy budget and advection effects and scaled by aerodynamic vapor transfer, following Brutsaert and Stricker (1979):

$$ET_a = (2\alpha_e - 1)\frac{\Delta}{\Delta + \gamma} Q_{ne} - \frac{\gamma}{\Delta + \gamma} \times 0.26(1 + 0.54\bar{u}_2) \times (e_s - e_a)$$

where α_e = 1.26 is the Priestley-Taylor coefficient (Priestley and Taylor, 1972), Δ is the slope of vapor pressure versus temperature curve (kPa °C^{-1}), Q_{ne} is the ratio of R_N to λ, γ is the psychometric constant (kPa °C^{-1}), $\bar{u}_2$ is the average wind speed (m s^{-1}) at 2 m reference height above the ground surface, and e_a and e_s are the actual and saturation vapor pressures (mmHg), respectively. The calculations of *in-situ* ET_a by the AA method were performed on a monthly basis during the study period over the Bahawal Nagar weather station. As noted earlier, meteorological parameters to force AA were obtained from PMD (see Table 1).

3.2. Crop evapotranspiration

For the crop water requirements, crop evapotranspiration (ET_c) was estimated via the use of a standard crop coefficient approach:

$$ET_c = ET_0 \times K_c \quad (5)$$

where ET_0 is the reference evapotranspiration and Kc is the relevant crop coefficient. ET_0 was estimated by using the meteorological data obtained from PMD, including minimum and maximum air temperature, solar radiation, relative humidity and wind speed for the study period, based on the methodology described by Allen et al.

Table 1
Description of remote sensing and meteorological datasets used to force the SEBS algorithm.

Variables	Product Source	Product Name	Spatial Resolution	Temporal Resolution	No of Products
LST/Emissivity	MODIS	MOD11A1	1000 m	Instantaneous	720
Surface Albedo	MODIS	MCD43B3	1000 m	8-day	276
NDVI	MODIS	MOD13A2	1000 m	16-day	138
LAI	MODIS	MOD15A2	1000 m	16-day	138
DEM	NASA	GTOPO30	1000 m	—	1
Meteorological variables	PMD (BahawalNagar)	Wind speed (m/s) Air pressure (Pa) Air temperature (K) Relative humidity (%) Solar radiation (W/m^2)	In-Situ	Hourly and daily	——

Note: LST, land surface temperature; NDVI, normalized difference vegetation index; LAI, leaf area index; DEM, digital elevation model; MODIS, Moderate Resolution Imaging Spectroradiometer; NASA, National Aeronautics and Space Administration online; PMD, Pakistan Meteorological Department.

(1998). The initial, mid and final stage K_c values for the major crops (Fig. 1b) identified in the region were derived from Ullah et al. (2001) and can be found in Fig. 4.

3.3. Gross canal water irrigation

The main source of surface irrigation to the study area is canal irrigation water from the Hakra branch canal, which diverts water to distributaries by regulating structures (Fig. 1a). There are a total of 17 distributaries from the Hakra branch canal, all of which are managed by Farmer Organizations (FOs). However, discharge measurement remains the responsibility of the Punjab Irrigation Department. A stream-gauging technique based upon the depth (stage) of water in each distributary is used to measure the discharge, with values at the inlet points of each distributary obtained from the Punjab Irrigation Department. These data were converted to gross canal water irrigation (IC_{gross}) depth on a monthly and seasonal basis.

3.4. Net canal water irrigation

Net canal water irrigation (IC_{net}), was calculated using the irrigation efficiency i.e. depth of water available at head of distributary multiplied by the irrigation efficiency (field and irrigation network efficiency). In order to incorporate irrigation network and field application losses, results from the study of Hussain et al. (2011) were used. According to that work, irrigation network efficiency and field application efficiency for the study region are 48% and 75%, respectively. When multiplied together, this results in an irrigation efficiency of 36%, which was adopted for the study region under consideration.

3.5. Net groundwater use

A GIS and remote sensing technique was used to estimate net groundwater use (IGW_{net}) from 2008 to 2014 on monthly basis. The approach has been shown to provide improvements over more conventional direct and indirect methods (Ahmad et al., 2005; Campos et al., 2013; Castaño et al., 2010). Satellite derived ET_a (see Section 3.1) maps were used as the main input for establishing the water balance in the unsaturated zone (root-zone), with the mass balance described as:

$$IGW_{net} = ET_a - IC_{net} - P \tag{6}$$

where ET_a (mm) is the remotely sensed actual evapotranspiration, IC_{net} (mm) is the net canal water irrigation and P (mm) is the precipitation amount.

3.6. Gross groundwater abstraction

IGW_{net} is the groundwater that is either retained in the root zone and used by the plants or evaporated. However, there is a significant amount of abstracted groundwater which is lost during conveyance of the water from the tube well to the field, as well as during application of water in the field. In order to incorporate irrigation network and field application losses, results from the study of Hussain et al. (2011) were used. According to that study, irrigation network efficiency and field application efficiency for the study region were 90% and 75%, respectively. Multiplying these values together yields an irrigation efficiency of about 68% for our study region, which is used to estimate the gross groundwater abstraction (IGW_{gross}).

3.7. Groundwater recharge

Normally, a water balance model that is tuned to the local conditions at the field scale is adopted to estimate groundwater recharge to the aquifer, which is defined as the difference between the gross amount of water entering and leaving the root zone. Precipitation provides part of the crop water needs, which is usually sufficient in more humid climates. However, agriculture in arid regions depends on artificial water supply by irrigation, in addition to precipitation. In the Hakra canal command area, the average annual rainfall in the region for the study period is approximately 318 mm $year^{-1}$. To supplement crop water needs, an considerable surface water supply is provided via the intensive irrigation network, which serves as the main source of water responsible for recharging the aquifer. Therefore, the groundwater recharge (GWR) calculated in this study is determined by the following equation:

$$\mathrm{GWR} = \left[(\text{Gross Irrigation} + \text{effective rainfall}) - \text{Net Irrigation}\right] \times \mathrm{K} \tag{7}$$

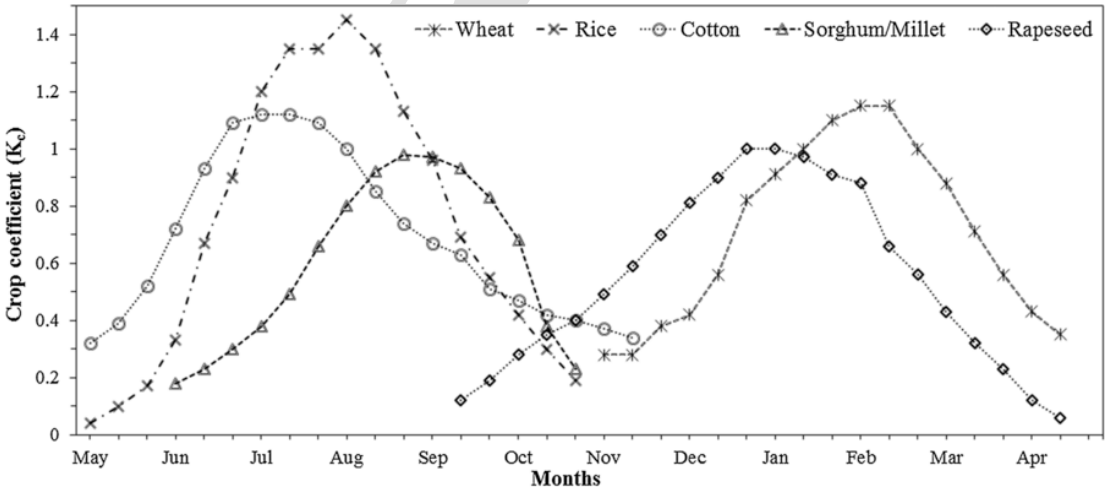

Fig. 4. Crop coefficient (K_c) of major crops in the Hakra canal command area.*(data Source:* Ullah et al., 2001*).*

where GWR is groundwater recharge in mm and K is a fraction (0.9) of the difference between the gross and net irrigation that recharges the aquifer (Awan et al., 2013). The deviation of this fraction from 1 accounts for operational losses and evaporation losses not contributing to percolation or groundwater recharge.

3.8. Net groundwater recharge

Groundwater recharge calculated using the methodology described in Section 3.7 contributes to the groundwater aquifer after time t. However according to local conditions, there is also discharge from the groundwater aquifer via an intensive network of tubewells. Considering aquifer discharge, the net groundwater recharge (GWR_{net}) becomes:

$$GWR_{net} = (\text{Groundwater Recharge} - \text{Groundwater Discharge}) \quad (8)$$

It should be noted that we are using the concept of gross irrigation and net irrigation for estimating the groundwater recharge (Eq. (7)) at the irrigation scheme level, which incorporates the conveyance (i.e., losses from major and minor canals, distributaries and water courses) and application losses. A similar concept has been implemented in the Khorezm region of Uzbekistan (Awan et al., 2013). Lateral groundwater flow in large irrigation schemes of the Indus basin are considered to be negligible on a long term basis, as revealed in a recent study by Shafeeque et al. (2016), so are not considered here.

4. Results and discussion

4.1. Validation of actual evapotranspiration (ET_a)

Monthly Surface Energy Balance System (SEBS) estimates of ET_a were extracted at the location of the weather station in the irrigation scheme in order to compare with ET_a derived from the Advection-Aridity (AA) method. As shown in Fig. 5a and b, time series and

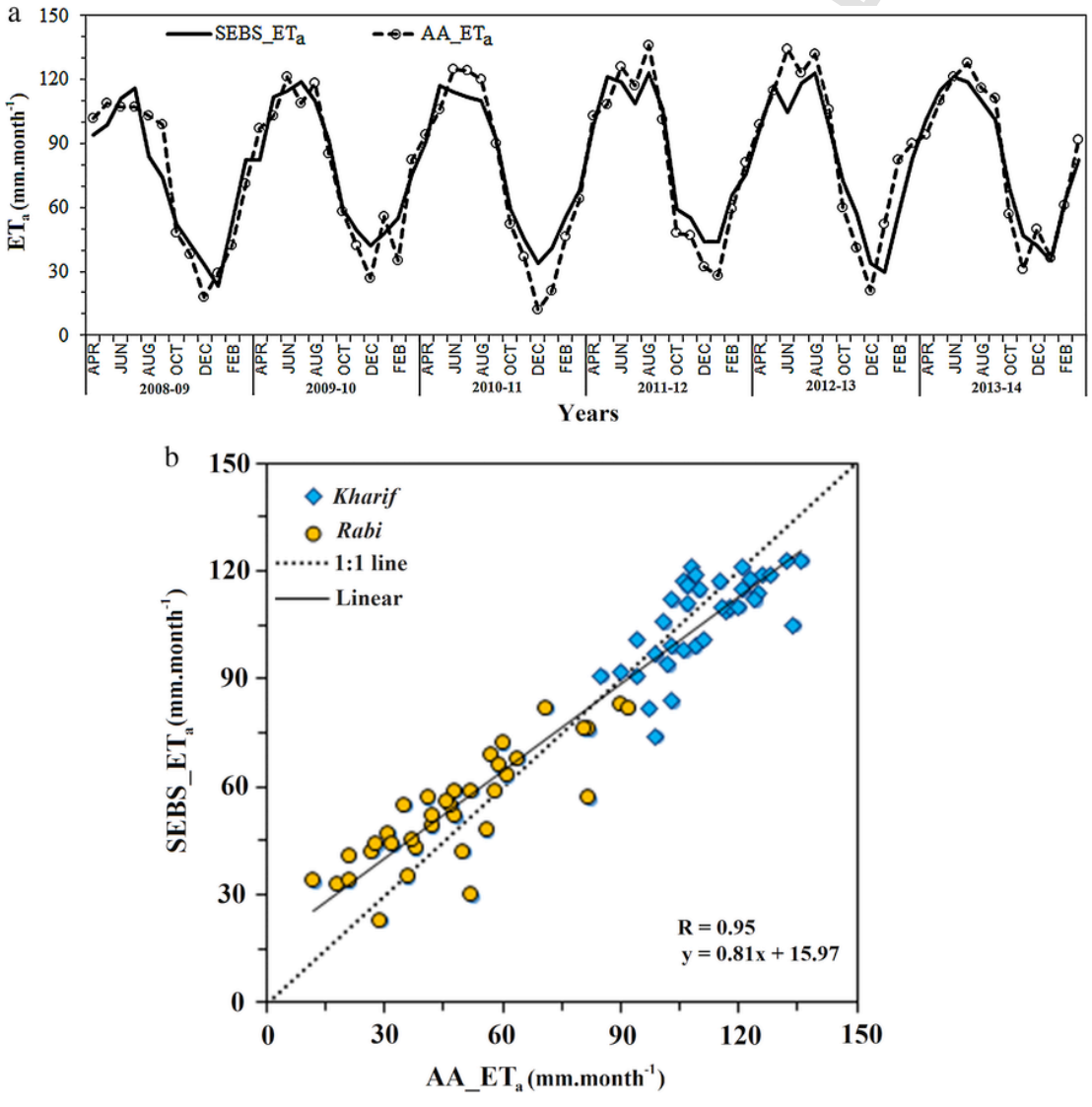

Fig. 5. Comparison between satellite-based ET_a from SEBS and ground measured ET_a from the advection-aridity (AA) method by means of (a) time series and (b) scatter plot analysis.

scatter plot comparisons reveal good agreement between the two methods. Such a level of similarity in monthly patterns of ET_a provide confidence in the use of the satellite derived SEBS product for more regional scale application. During the *Kharif* (Apr-Sep) season, ET_a estimated by AA was slightly higher than SEBS, while SEBS ET_a exceeded AA during *Rabi* (Oct-Mar). This variation may result from differences in climatic conditions, land use practices and water availability between the seasons, as well as the sensitivity of SEBS model to both these and meteorological forcing (Ershadi et al., 2013a; Liaqat et al., 2015). The overall agreement is further reflected in the scatter plot analysis of Fig. 5b, which shows a strong Pearson correlation (R) of 0.95 between SEBS and AA ET_a for monthly values from 2008 to 2014.

Interestingly, a statistical analysis between ET_a from the two approaches on a seasonal basis depicted relatively large differences (Table 2). Statistical parameters including R (0.69), Nash–Sutcliffe model efficiency (NSE) (0.28), percentage bias (PBIAS) (−3.85%) and root mean square error (RMSE) (10.66 mm) were estimated for the *Kharif* season compared to 0.84, 0.63, 10.65% and 12.21 mm for *Rabi* season, and 0.95, 0.90, 0.56% and 11.46 mm on an annual basis, respectively. When the direction of the error was considered, the negative and positive PBIAS values reflected that SEBS results were under- and over-estimated, respectively, compared with AA measurements. The pattern of over- and under-estimation were induced by the seasonal changes in important input variables, such as land surface and air temperature, wind speed, and roughness parameterization in SEBS, which are known to be highly sensitive variables for this particular model (Ershadi et al., 2013a; Gibson et al., 2011). Differences in results between the *Kharif* and *Rabi* periods has been replicated in a number of previous research efforts (Liaqat et al., 2015; Liu et al., 2006), with the authors suggesting that the performance of the AA method is relatively poor during extreme dry or in wet environmental conditions. Recently, Liaqat et al. (2015) validated the SEBS model for the Indus Basin Irrigation System, including the Hakra canal command area, and reported that SEBS ET_a was underestimated by approximately −0.15 mm day^{-1} during the summer period, and overestimated by 0.23 mm day^{-1} during the winter period. The authors argued that the SEBS model includes the inherent heterogeneity in ET_a values at large spatial scales, when compared with those obtained from conventional methods or with the actual water consumption at field or point scale. Therefore, the overall differences of ET_a on an annual scale in the current study seem more than acceptable, considering the inherent errors in the satellite data, as well as the scale difference between the MODIS 1 km pixel size and point scale meteorological measurements (Byun et al., 2014; Choi et al., 2011).

The close correspondence between both approaches suggest that AA is also a useful method to account for actual water losses from semi-arid to arid regions at point scales, and can be used to validate pixel by pixel spatial scale models such as SEBS. Its practical reliability in estimating the actual, wet environment and potential ET using relatively simple meteorological requirements may recommend it as a basis for water resources planning and management at point or field scales, especially in rural river basin characterized with limited data resources.

Table 2
Statistical comparison between seasonal and annual average ET_a estimated by SEBS and the advection-aridity (AA) method.

Season	Mean		Standard Deviation		Goodness-of-fit measures			
	SEBS ET_a	AA ET_a	SEBS ET_a	AA ET_a	R	NSE	PBIAS	RMSE
	(mm)	(mm)	(mm)	(mm)	–	–	(%)	(mm)
Kharif	106.81	111.08	12.59	12.74	0.69	0.28	−3.85	10.66
Rabi	53.67	48.50	15.64	20.46	0.84	0.63	10.65	12.21
Annual	80.24	79.80	30.24	35.77	0.95	0.90	0.56	11.46

4.2. Quantification of water resources management (WRM) components

The quantification of the nine WRM components on a monthly, seasonal and annual basis are summarized in Table 3 through Table 11. Results show that actual evapotranspiration (ET_a) during the *Kharif* season was 33% higher than in the *Rabi* season, while values on a yearly basis showed relatively minor change (Table 3). High ET_a during *Kharif* was due to the larger availability of water in the irrigation system coupled with higher crop water requirements. The monthly variation in ET_a ranged between 23 mm (January) to 123 mm (Aug), with an annual average value of 963 mm over the six year study period (2008–2014). The peak ET_a rates were observed during the months of May to August and corresponded to rice crop areas. The lowest ET_a occurred during the months of December and January, due to decreased crop water requirements and little or no water supplies in the irrigation scheme (Ahmad et al., 2005).

The results of crop evapotranspiration (ET_c) showed less significant variation between the years, although large differences were observed on a seasonal basis (Table 4). High ET_c during *Kharif* was due to a high reference evapotranspiration and eventually high crop water requirements. Maximum ET_c (>150 mm) occurred during May to August, whereas the lowest values (<55 mm) were from December to January, with an annual average of 1391 mm (which is about 428 mm larger than average ET_a on annual basis). The reason behind this large difference is the lower availability of irrigation water (from all sources) to the crops, relative to their actual requirements. Irrigation schemes in the Indus basin were designed for 70% cropping intensities. However, after the green revolution of the 1960s, the cropping

Table 3
Distribution of actual evapotranspiration (mm) in Hakra from 2008 to 2014.

Seasonal	*Kharif*						*Rabi*					
Annual	A	M	J	J	A	S	O	N	D	J	F	M
2008–09	94	99	111	116	84	74	52	43	33	23	52	82
2009–10	82	112	115	119	110	91	59	49	42	48	55	76
2010–11	91	117	114	112	110	92	59	45	34	41	56	68
2011–12	99	121	119	109	123	106	59	55	44	44	66	76
2012–13	97	117	105	118	123	98	72	57	34	30	57	83
2013–14	101	115	121	119	110	101	69	47	42	35	63	82
Annual Average	94	114	114	116	110	94	62	49	38	37	58	78
Seasonal Average	641 (66.5%)						322 (33.5%)					

Table 4
Distribution of crop evapotranspiration (mm) in Hakra from 2008 to 2014.

Seasonal	*Kharif*						*Rabi*					
Annual	A	M	J	J	A	S	O	N	D	J	F	M
2008–09	152	159	157	157	143	129	88	71	53	55	80	128
2009–10	147	163	161	159	148	125	88	73	55	86	88	129
2010–11	144	166	171	154	150	130	95	79	55	11	90	134
2011–12	153	168	156	157	156	131	98	80	53	62	91	113
2012–13	149	165	154	153	162	126	90	75	55	52	82	129
2013–14	144	160	151	156	156	121	87	72	50	56	85	124
Annual Average	148	164	158	156	153	127	91	75	54	54	86	126
Seasonal Average	906 (65%)						485 (35%)					

intensities increased to more than double that amount (Ahmad et al., 2014; Awan et al., 2016). Despite this increase, the canal water supplies remained the same, which resulted in a large gap between supply and demand that has now caused severe water scarcity in the region. The difference can also be attributed to the area average based estimation of ET_a that included non-crop areas, resulting in lower ET_a values compared with the ET_c point based calculations for cropped area. Moreover, unreliable surface irrigation supply in both cropping seasons, restricted groundwater pumping to reduce cost as well as to avoid the salinity effect on crops in saline areas: all of which may contribute to the observed differences between ET_a and ET_c. Overall, based on the total Hakra canal command area, it was estimated that around 3.8 mm day^{-1} of water was required from the available water resources to meet the root zone crop water requirement, with an approximate distribution of 5 mm day^{-1} during *Kharif* season and 2.7 mm day^{-1} during *Rabi* season.

In terms of gross canal water irrigation (IC_{gross}) depth, maximum IC_{gross} was 678 mm during the 2011–12 cropping year, whereas the minimum was 608 mm during the 2009–10 cropping year, with an average annual canal water supply of 1.75 mm day^{-1} for the Hakra (Table 5). Water supply during *Kharif* season was 14% more than *Rabi* season, since the irrigation authorities close the canals during December and January for removal of accumulated silt deposition (Ahmad et al., 2005). Overall, around 2 mm day^{-1} water was available to the area during the *Kharif* season, and around 1.50 mm day^{-1} during the *Rabi* season. Net canal water use (IC_{net}) results (Table 6) were varied according to IC_{gross} depths. Against IC_{gross} of 1.75 mm day^{-1} for the entire season, the average IC_{net} was only 0.55 mm day^{-1}, 0.72 mm day^{-1} and 0.63 mm day^{-1} during *Rabi*, *Kharif* and on annual basis, respectively (Table 6).

Rainfall results are shown in Table 7. Since the precipitation varied between 198 mm year^{-1} and 502 mm year^{-1}, with an average of 318 mm year^{-1} during 2008–2014, the sum of rainfall and IC_{net} was insufficient to meet the ET_c (Table 4) i.e., crop water requirements. Monthly average rainfall varied largely between 1 mm and 99 mm, presenting a maximum occurrence of more than 45 mm month^{-1} during the monsoon season (June to September), with seasonal averages of 14% *(Rabi)* and 86% *(Kharif)* of the total rainfall amount.

As the sum of IC_{net} and rainfall for the average of six year study period was only 548 mm (36% of ET_c), farmers rely on groundwater use to meet residual crop water requirements. On average, 680 mm was abstracted from the groundwater aquifer, which varied between 593 mm and 806 mm on a yearly basis, with a 39% and 61% proportion during *Rabi* and *Kharif* season, respectively (Table 8). The fluctuations in groundwater abstraction between 0 mm to 143 mm in various months were mainly controlled by rainfall pattern and crop water requirements, as discussed above. The lowest groundwater abstraction amounts occurred during the months of September (27 mm) and December (20 mm), which could be due to high monsoon rainfall and sowing of less water demanding crops, respectively. Net groundwater use (IGW_{net}), estimated after incorporating the efficiencies (see Sections 3.4 & 3.5) was 463 mm year^{-1} (Table 9) on average during the study period, which was almost twice the usage of water from the canal water supply. Unlike surface water use from canals, the maximum groundwater use in the month of May was due to the cultivation of rice, as well as insufficient rainfall and canal water availability.

Table 5
Distribution of canal water use (mm) in Hakra from 2008 to 2014.

Seasonal	*Kharif*						*Rabi*						
Annual	A	M	J	J	A	S	O	N	D	J	F	M	Total
2008–09	61	57	64	67	64	68	36	68	62	7	49	35	636
2009–10	63	70	63	72	66	50	33	66	46	0	30	49	608
2010–11	47	46	64	66	72	63	41	68	63	4	65	69	668
2011–12	70	70	69	66	56	20	53	69	71	10	67	57	678
2012–13	58	44	56	68	69	51	63	66	60	0	37	60	631
2013–14	58	68	65	69	52	62	52	61	43	0	46	39	615
Annual Average	60	59	64	68	63	52	46	66	58	4	49	52	639
Seasonal Average	366 (57%)						274 (43%)						

Table 6
Distribution of net canal water use (mm) in Hakra from 2008 to 2014.

Seasonal	*Kharif*						*Rabi*						
Annual	A	M	J	J	A	S	O	N	D	J	F	M	Total
2008–09	22	20	23	24	23	24	13	25	22	2	18	13	229
2009–10	23	25	22	26	24	18	12	24	16	0	11	18	219
2010–11	17	17	23	24	26	23	15	24	23	1	23	25	241
2011–12	25	25	25	24	20	7	19	25	25	4	24	21	244
2012–13	21	16	20	24	25	19	23	24	22	0	13	22	227
2013–14	21	25	23	25	19	22	18	22	15	0	17	14	221
Annual Average	22	21	23	25	23	19	17	24	21	1	18	19	230
Seasonal Average	132 (57%)						99 (43%)						

Table 7
Distribution of rainfall (mm) in Hakra from 2008 to 2014.

Seasonal	*Kharif*						*Rabi*						
Annual	A	M	J	J	A	S	O	N	D	J	F	M	Total
2008–09	9	36	54	51	39	9	0	0	8	14	12	14	246
2009–10	7	2	24	111	1	57	0	0	0	1	5	1	209
2010–11	0	3	30	67	68	15	0	0	5	0	9	1	198
2011–12	36	16	76	11	115	242	0	0	0	3	3	0	502
2012–13	22	5	7	36	35	177	16	0	8	4	6	42	358
2013–14	14	11	82	56	35	91	47	4	3	4	6	42	395
Annual Average	15	12	46	55	49	99	11	1	4	4	7	17	318
Seasonal Average	275 (86%)						43 (14%)						

Table 8
Distribution of gross groundwater abstractions (mm) in Hakra from 2008 to 2014.

Seasonal	*Kharif*						*Rabi*						
Annual	A	M	J	J	A	S	O	N	D	J	F	M	T
2008–09	92	62	50	61	33	60	57	27	6	10	34	82	5
2009–10	77	124	100	0	125	24	69	38	37	70	57	85	8
2010–11	109	143	90	31	24	79	64	31	9	58	35	62	7
2011–12	55	117	26	110	2	0	58	45	27	55	57	82	6
2012–13	79	141	114	85	92	0	50	49	7	38	56	28	7
2013–14	97	116	23	56	84	0	9	31	35	46	59	38	5
Annual Average	85	117	67	57	60	27	51	37	20	46	50	63	6
Seasonal Average	414 (61%)						266 (39%)						

Table 9
Distribution of net groundwater use (mm) in Hakra from 2008 to 2014.

Seasonal	*Kharif*						*Rabi*						
Annual	A	M	J	J	A	S	O	N	D	J	F	M	Total
2008–09	63	42	34	41	22	41	39	18	4	7	23	56	390
2009–10	53	85	68	0	85	16	47	26	25	47	39	58	548
2010–11	74	97	61	21	17	54	44	21	6	40	24	42	500
2011–12	37	80	18	75	1	0	40	30	19	37	39	56	431
2012–13	54	96	77	58	63	0	34	33	5	26	38	19	503
2013–14	66	79	15	38	57	0	6	21	24	31	40	26	403
Annual Average	58	80	46	39	41	19	35	25	14	31	34	43	463
Seasonal Average	281 (61%)						182 (39%)						

The total annual average groundwater recharge estimated by using Eq. (7) was 565 mm, with an approximate 40 mm variation over the study period (Table 10). Maximum monthly groundwater recharge (>50 mm) occurred from April to August, while it reduces in other months (<50 mm). The seasonal averages during *Rabi* and *Kharif* were 235 mm and 330 mm, which reflected 42% and 58% of the total annual values, respectively. It is worth noting that the elevated field boundaries (bunds) and moderately elevated slope in the region help to prevent runoff, even during the high intensity rains that occur in the monsoon period (Ahmad et al., 2005).

The results of net groundwater recharge show that there is more groundwater abstraction than groundwater recharge (Table 11). Negative and positive values were observed in both *Rabi* and *Kharif* seasons, with an annual average net groundwater recharge of −115 mm year^{-1} during the last six years. The negative value shows that water fluxes above or at the surface are higher than subsurface fluxes, which are causing decline of groundwater levels. Although the average values are only −115 mm year^{-1}, some months have high groundwater recharge values (e.g., September, November and December) while all others months have high discharge values. Positive groundwater recharge during these months was likely caused by either high rainfall amount observed during the study period (See Table 7) or due to the initial sowing period of wheat crop, which has reduced water requirements in winter months (November and December).

Overall, the decline of groundwater was −32 mm (27.5%) and −83 mm (72.5%) of total annual groundwater recharge values during *Rabi* and *Kharif* seasons, respectively. To verify these estimates of net groundwater recharge, we determined the trends of depth to groundwater (DTGW) measured from eleven observation wells installed across the project area. Fig. 6 illustrates the increase in DTGW for the period 2008–2014 over all observation wells except well #8, where a slight decline in DTGW was observed. These results of groundwater overdraft are in accord with recent studies (Cheema et al., 2014; Shafeeque et al., 2016), and can be attributed to changes in cropping pattern and intensities, as well as low irrigation efficiencies in the region. An improvement in these variables is under discussion for the sustainability of groundwater recharge: in particular, changes in cropping pattern, which is an alternative option to reduce the groundwater extraction. However, the marketing of a new crop is a major obstacle for farmer uptake. An examination of these complex scenarios requires a comprehensive and inter-disciplinary approach, where rigorous socio-economic analysis should be included.

Table 10
Distribution of groundwater recharge rate (mm) in Hakra from 2008 to 2014.

Seasonal	*Kharif*						*Rabi*						
Annual	A	M	J	J	A	S	O	N	D	J	F	M	Total
2008−09	62	51	51	56	46	56	38	47	37	7	38	44	532
2009−10	59	76	65	41	74	36	39	49	37	20	34	53	583
2010−11	59	68	63	47	49	59	42	48	39	19	48	58	597
2011−12	56	74	48	70	33	11	48	53	49	22	55	57	574
2012−13	56	66	65	63	66	30	51	52	37	11	37	43	577
2013−14	62	73	44	56	54	36	32	44	35	14	43	34	526
Annual Average	59	68	56	56	54	38	42	49	39	16	43	48	565
Seasonal Average	330 (58%)						235 (42%)						

4.3. Spatial patterns of WRM components

Three hydrological years, i.e., 2008–09, 2011–12 and 2013-14, were selected to represent the spatial distribution of annual average actual evapotranspiration, net groundwater use, groundwater recharge and net groundwater recharge estimated using the satellite datasets across the Hakra canal command areas (Figs. 7 and 8). The variations in SEBS estimated ET_a ranged between 400 to 1300 mm year^{-1} on average in the cultivated area of the basin (Fig. 7a). Normally, the variations in intra-annual ET_a can be attributed to the amount of irrigation water supplied from different resources, cropping practices, underlying soil types and atmospheric boundary layer settings in the region. However, these conditions did not change significantly during the study period (Awan and Ismaeel, 2014). Thus, only minor variations in spatial ET_a occurred for all of the selected years. Higher ET_a were mostly observed in rice growing areas (see Fig. 1b), which are located near the head of distributaries (see Fig. 1a), resulting in greater proximity to canal water supplies. A large swath of low ET_a values can be seen at the tail end of the canal irrigation, where less water demanding crops (Gram-Millet) are cultivated due to the presence of sandy soil (which causes high seepage to groundwater). Generally, the primary reasons for low ET_a can be attributed to the reduction in canal water supply and farmer restrictions to the extensive groundwater pumping to reduce cost and to avoid salinity effect in tail areas.

Pixel based net groundwater use for meeting the crop water demands in the region show large spatial variation ranging from 0 mm to 800 mm year^{-1} (Fig. 7b) over the study period. The fluctuations in groundwater use were generally induced due to differences in rainfall patterns, as the water supplies from canals remained similar over the years. The highest groundwater use (>700 mm year^{-1}) was observed in rice and cotton cultivated areas during the first (2008-09) and last (2013-14) cropping year. This is because the irrigation network supplies an insufficient amount of water, and farmers ultimately shift to good quality groundwater abstraction in conjunction with rainfall to fulfil crop needs. Minimum groundwater use was seen across tail-end areas, where the cost of groundwater abstractions is greater and the quality of groundwater is poor (Awan et al., 2016).

Fig. 8a presents the average annual groundwater recharge, which varies from 0 mm to 750 mm year^{-1}. The areas having higher cropping intensities are attributes to greater surface water supplies. Scat-

Table 11
Distribution of net groundwater recharge rate (mm) in Hakra from 2008 to 2014.

Seasonal	*Kharif*						*Rabi*						
Annual	A	M	J	J	A	S	O	N	D	J	F	M	Total
2008−09	−31	−12	1	−5	14	−4	−19	20	32	−3	4	−38	−41
2009−10	−19	−48	−35	41	−51	12	−31	11	0	−49	−23	−32	−223
2010−11	−51	−76	−27	16	25	−19	−22	19	30	−39	12	−4	−136
2011−12	1	−43	22	−40	31	11	−11	8	21	−33	−2	−25	−60
2012−13	−23	−75	−49	−22	−26	30	1	3	29	−27	−19	15	−165
2013−14	−35	−43	21	0	−29	35	23	13	0	−33	−16	−4	−64
Annual Average	−26	−49	−11	−2	−6	11	−10	12	19	−31	−7	−15	−115
Seasonal Average	−83 (72.5%)						−32 (27.5%)						

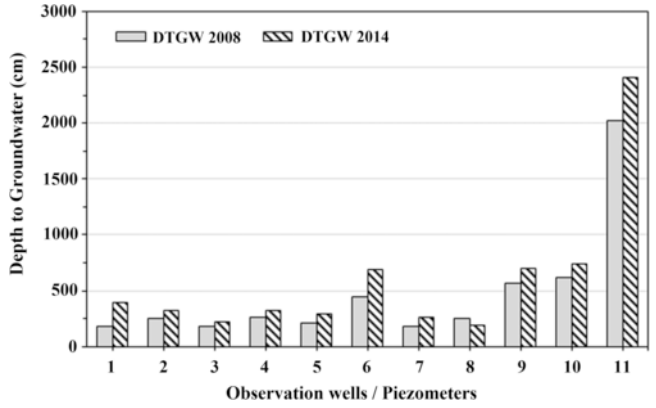

Fig. 6. Changes in groundwater table depth (GWTD) measured at the start (2008) and end (2014) of the study period from 11 systematically distributed observation wells in the study area (n.b. for identification of observation wells, the reader is referred to Fig. 1).

tered patterns of groundwater recharge were also observed in those areas having wheat-cotton or wheat-rice rotations. Desert or barren areas have no groundwater recharge, while in all other areas, groundwater recharge was occurring uniformly with values ranging from 350 mm to 500 mm year^{-1}.

The groundwater recharge and abstraction were used to estimate the net aquifer depletion (or replenishment) i.e., net groundwater recharge for each pixel. The estimated net groundwater recharge ranged from −400 to 400 mm year^{-1}, with negative and positive values indicating areas depleting and replenishing, respectively (Fig. 8b). Among the selected hydrological years, the depletion in groundwater table during 2008–09 and 2013–14 were higher than for 2011–12, which showed mostly positive values in areas less vulnerable to groundwater depletion. On average, the net groundwater depletion during all six years was found to be −115 mm year^{-1} (Table 11), which is in accord with the results of −121 mm year^{-1} groundwater depletion found for the entire Indus Basin Irrigation System in Cheema et al. (2014). More recently, Shafeeque et al. (2016) reported an average of −91 mm year^{-1} net recharge, which was estimated using the Soil and Water Assessment Tool (SWAT) in the Hakra branch canal for the period 2006–2011.

4.4. Establishing a correlation among identified WRM components

Pearson correlation (R) at two different significance levels (*p*-value of 0.01 and 0.05) were calculated between the different WRM components during both the *Kharif* and *Rabi* seasons, with results presented in Tables 12a and 12b, respectively. ET_a was positively correlated with all components except net groundwater recharge. It showed a good correlation of 0.67 and 0.87 with ET_c during *Kharif* and *Rabi* seasons, respectively, at a significance level of $p < 0.01$. The significant relationship between ET_a and ET_c likely reflects the high diurnal cycle of solar energy in this region, which is a required variable for both estimation approaches. Generally, the correlation result shows a very weak relationship ($R \leq 0.16$) between ET_a and irrigation water components, e.g., canal (IC_{gross} and IC_{net}), groundwater (IGW_{gross} and IGW_{net}) and rainfall, during *Kharif* season (Table 12a) in comparison to a slightly better and significant correlation ($R \geq 0.32$) for the *Rabi* season (Table 12b). Interestingly, the correlations of ET_c with other components were slightly better in *Kharif* than in *Rabi*. A possible explanation for this difference is that ET_c calculations are at a point level and are mostly kept uniform for the entire region, whereas ET_a is estimated pixel by pixel and changes even for the same crops. Seasonal differences in correlations could be related to fluctuating rainfall patterns, variations in solar radiation, unreliable surface water supplies and changes in groundwater extraction between seasons. The results presented in Section 4.2 reveal that groundwater fulfills most of the crop water requirements, while the moderate positive correlation ($R \geq 0.49$) between ET_c and groundwater use at a significance level of $p < 0.05$, indicates that the relationship between demand based water supply and crop water requirement in the system are occurring at the same time and place.

Ground water use has a very weak ($R \leq 0.06$) or negative ($R \leq -0.24$) correlation with canal water use during *Kharif* and *Rabi* seasons, respectively. This discrepancy was expected, as water supply from the canals are provided at a constant rate without information on actual crop water need (supply based irrigation system), while farmers pump the groundwater depending upon crop use (demand base ground water supply). An increase in rainfall amount decreased the use of groundwater, as their relationship showed significant negative correlation ($R \leq -0.36$) throughout the year, while the impact of rainfall was less or non-significant on canal water supply, which is delivered to fields at a fixed rate, as mentioned above. The various water availability components behave differently in their contribution to groundwater recharge. During the *Kharif* season, maximum groundwater recharge was contributed from pumped groundwater and rainfall ($R \geq 0.89$; Table 12a) followed by canal water supplies ($R \geq 0.47$). This was because of high standing water requirements for rice paddies, which are usually fulfilled from a combination of all irrigation resources, including groundwater abstraction. On the contrary, the canal water losses during the *Rabi* season are mainly contributing to groundwater recharge, as observed from their strong and significant correlation ($R \geq 0.89$; Table 12b). Rainfall significantly contributed to the groundwater recharge and net recharge during *Kharif* season, reflected in a strong R value of 0.89 and 0.72, compared with weaker R values of 0.15 and 0.26 during the *Rabi* season, respectively. Since net groundwater recharge was estimated as the difference between groundwater discharge and recharge, the results show that its values were negatively and positively affected with groundwater pumping and canal water supplies or net rainfall amount, respectively. This was due to the fact that losses from groundwater use were less, compared with those from combined canal network and field application losses. Overall, the identified major source of net ground water recharge were rainfall and canal irrigation, with correlations of 0.72 (Table 12a) and 0.75 (Table 12b) during the *Kharif* and *Rabi* seasons, respectively.

The analysis above describes the discrete interactions of various water resources management components on a seasonal basis and does not sufficiently reflect the variations between incoming and outgoing water mechanism. To examine this, we plotted the changes in monthly ET_a and net groundwater recharge against the combination of irrigation inputs (Fig. 9). The relationship of ET_a increases with changing source of water from supply based irrigation to demand based irrigation (Fig. 9a–b), which means that neither canal, nor groundwater and rainfall are sufficient to meet ET_a. A comparison of changes in ET_a with gross canal water plus rainfall amount yielded a correlation (R) of 0.69 (Fig. 9a), which shows the lack of available water from both resources to account for ET_a at its potential rate. By replacing the canal supplies with groundwater, an R of 0.94 was observed with a slope value close to the 1:1 line (Fig. 9b), indicating that groundwater use is more significant in addressing the crop water requirement in this type of semi-arid environment. In Fig. 9c, a positive slope of 0.41 with a moderate R of 0.57 indicated the maximum net groundwater recharge occurred in the system via the combined loss from canal water and rainfall amount. However, the comparison

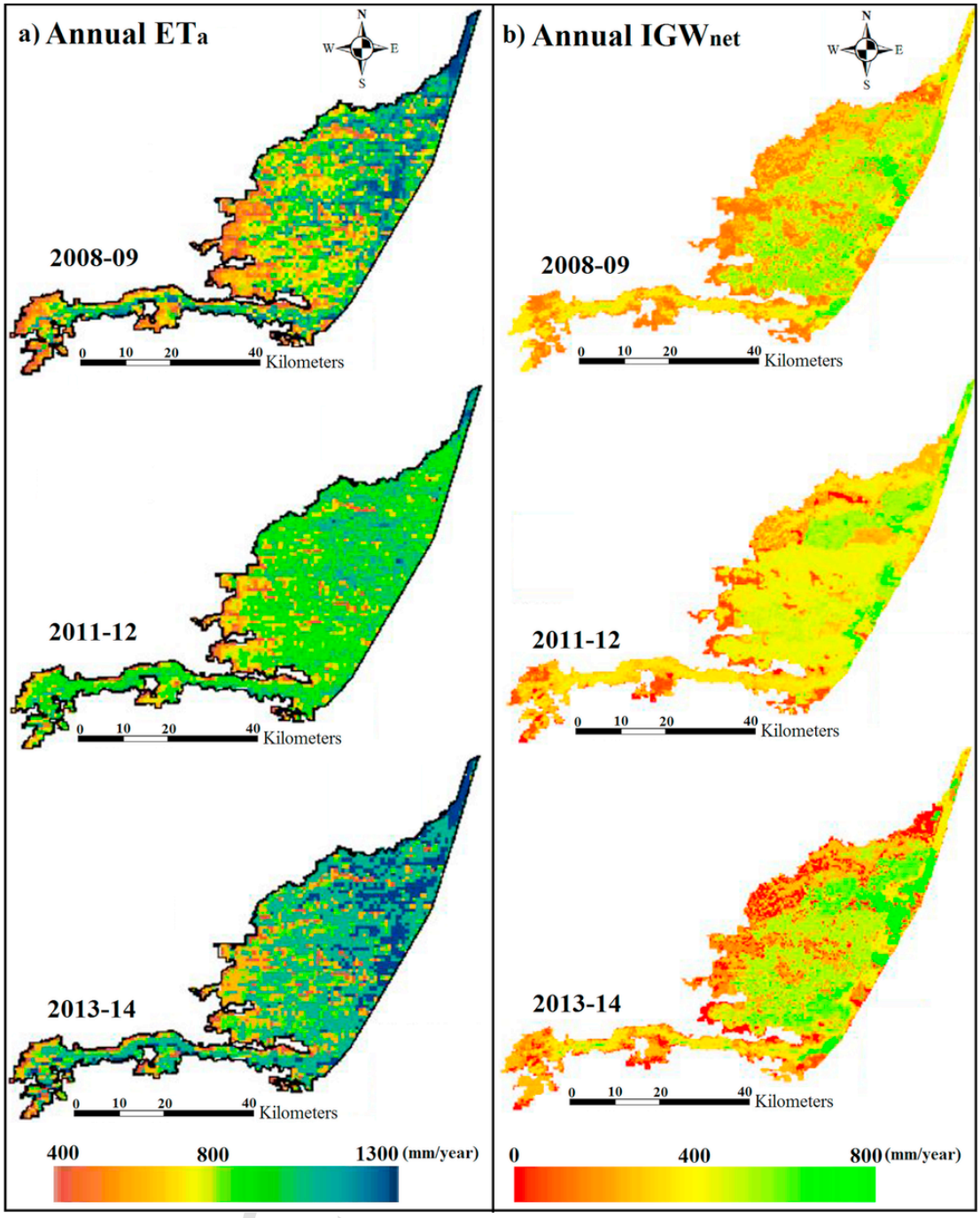

Fig. 7. Spatial distribution of cumulative annual (a) actual evapotranspiration (ET_a) and (b) net groundwater use (IGW_{net}) during three selected hydrological years in the Hakra canal command area.

of net groundwater recharge with gross groundwater in addition to rainfall amount (Fig. 9d) revealed a negative relationship with an R of −0.50, which suggests that groundwater abstraction collectively with rainfall is more representative of ET_a or ET_c and is generally not available for groundwater replenishment in this region.

The correlation analysis explored above is useful to understand the linkages between different WRM components in the complex irrigation system, which depends not only on surface water but also groundwater supplies. Further, there is an ongoing debate on resilient groundwater levels for the sustainability of irrigated agriculture. Groundwater levels depends on recharge and discharge mechanisms, and if management authorities in the region or in similar areas wish to establish resilient groundwater levels, the exercise will be useless unless it is supported by detailed information on correlation between different WRM components.

5. Conclusion

Modern satellite techniques and state-of-the-art tools help in the quantification and assessment of interrelationships between key water

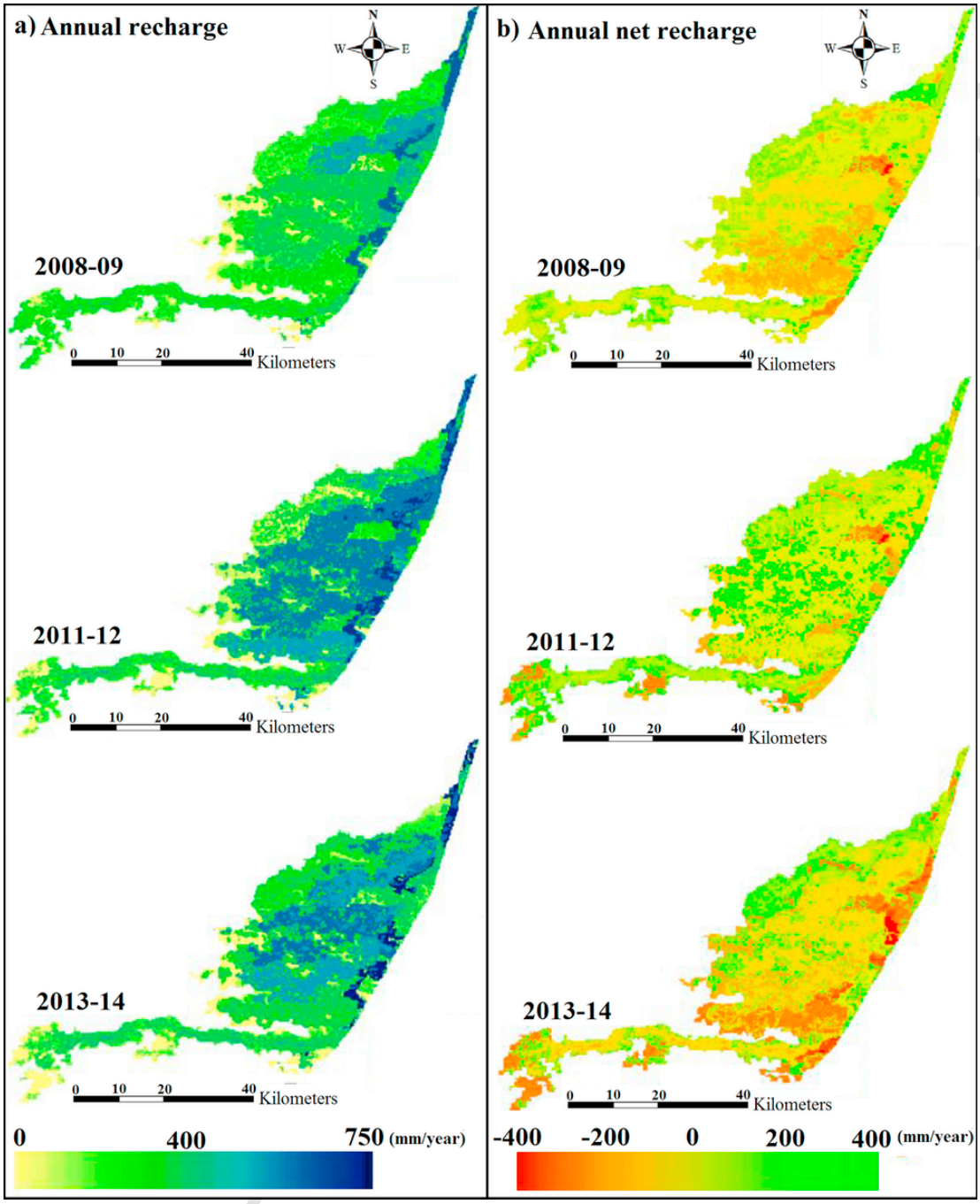

Fig. 8. Spatial distribution of cumulative annual (a) groundwater recharge rate as well as (b) net groundwater recharge rate during three selected hydrological years in the Hakra canal command area.

resources management (WRM) components. The methodology explored here not only captured the variability between the surface WRM components, but also identifies a strong relationship between surface and groundwater interactions. The evaluation of SEBS derived ET_a were shown to be satisfactory indicators of spatial and temporal variability, with R (0.95), NSE (0.90), PBIAS of 0.56% and RMSE (11.46 mm year^{-1}) when compared with advection-aridity derived ET_a from ground based measurements.

The irrigation system in the Indus basin depends largely on surface and groundwater. Results indicate that groundwater contributes 48% of the crop water requirement, representing an integral component of the water cycle that cannot be ignored for managing such large irrigation schemes. The approach developed here is adaptable to readily map pixel-based annual groundwater abstraction in the region, which was shown to range between 573 and 806 mm during the study period of 2008–2014. Groundwater recharge and discharge depends on surface water use, which means that there is a strong interaction between these two resources. The average groundwater abstraction of 680 mm year^{-1} was 20% more than groundwater recharge (565 mm year^{-1}), revealing serious flaws in past groundwater management policies. With little change in subsequent years, it is clear that the groundwater use and continued management policies cur-

Table 12a
Correlation matrix of water resources management components through Pearson correlation during *Kharif* season.

	ET_a	ET_c	IC_{gross}	IC_{net}	IGW_{gross}	IGW_{net}	Rainfall	Recharge	Net Recharge
ET_a	1								
ET_c	0.67**	1							
IC_{gross}	0.16	0.31	1						
IC_{net}	0.16	0.31	1.00**	1					
IGW_{gross}	0.09	0.52**	0.06	0.06	1				
IGW_{net}	0.09	0.52**	0.06	0.06	1.00**	1			
Rainfall	0.15	−0.39*	−0.42*	−0.42*	−0.81**	−0.81**	1		
Recharge	0.15	0.59*	0.47**	0.47**	0.91**	0.91**	0.89**	1	
Net Recharge	−0.06	−0.45*	0.15	0.15	−0.98**	−0.98**	0.72**	−0.81**	1

Table 12b
Correlation matrix of water resources management components through Pearson correlation during *Rabi* season.

	ET_a	ET_c	IC_{gross}	IC_{net}	IGW_{gross}	IGW_{net}	Rainfall	Recharge	Net Recharge
ET_a	1								
ET_c	0.87**	1							
IC_{gross}	0.32*	0.29	1						
IC_{net}	0.32*	0.29	1.00**	1					
IGW_{gross}	0.54**	0.49**	−0.24	−0.24	1				
IGW_{net}	0.54**	0.49**	−0.24	−0.24	1.00**	1			
Rainfall	0.44**	0.34*	0.02	0.02	−0.36*	−0.36*	1		
Recharge	0.57*	0.53**	0.89**	0.89**	0.24	0.24	0.15	1	
Net Recharge	−0.19	−0.16	0.75**	0.75**	−0.82**	−0.82**	0.26	0.35*	1

* Correlation is significant at 0.05 level.

** Correlation is significant at 0.01 level.

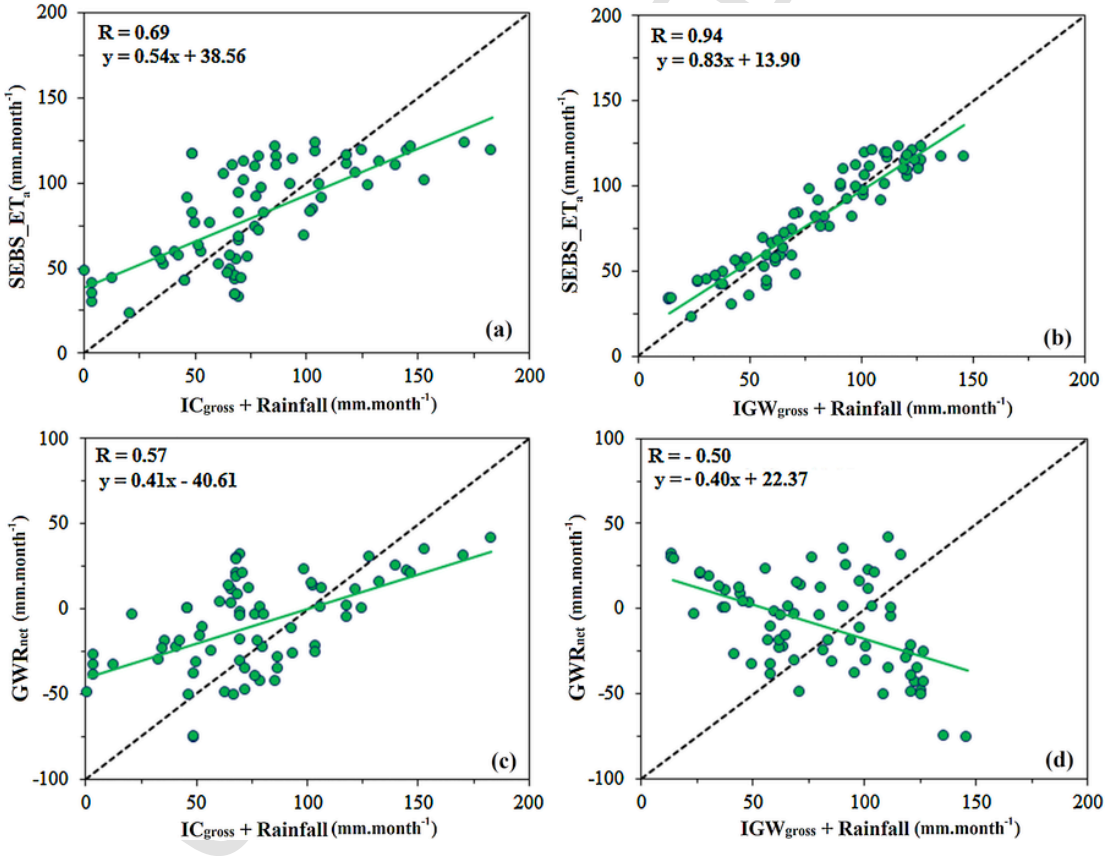

Fig. 9. Relationship of mean monthly irrigation input parameters with monthly average (a–b) actual evapotranspiration (ET_a) and (c–d) net groundwater recharge (GWR_{net}) rates.

rently in place are not sustainable. Quantification of key WRM components suggested large seasonal differences. However the annual differences were not shown to be significant, at least for the period studied. Detailed spatial maps and the estimated average groundwater depletion (−41 mm $year^{-1}$ to −223 mm $year^{-1}$) present as useful indicators to negotiate and maintain the aquifer sustainability.

Correlation between WRM components was seen to be stronger during the *Rabi* season due to low crop evapotranspiration and sufficient surface water supplies. Monthly ET_a were significantly ($p < 0.01$) impacted by changes in groundwater abstraction, while net groundwater recharge received a significant contribution from canal irrigation supplies and from rainfall. The correlation analysis explored in this study can be used to guide the determination of more resilient groundwater levels for using the available resources in a reasoned and sustainable manner. Through exploring such spatial interactions, the proposed methodology can provide important information on surface-groundwater interactions that can guide policy makers to sustainably exploit existing water resources.

Conflict of interest

The authors declare that they have no conflicts of interest.

Acknowledgments

This research was supported by Space Core Technology Development Program through the National Research Foundation of Korea (NRF) funded by the Ministry of Science, ICT and Future Planning (NRF-2014M1A3A3A02034789). Matthew McCabe was supported by the King Abdullah University of Science and Technology, Saudi Arabia. The authors acknowledge the various NASA services for providing free and unrestricted access to MODIS products. We are also grateful to Mr. Habib Ullah Bodla, Chief of the Punjab Monitoring and Implementation Unit, for providing us discharge data for the different canals in the study region.

References

Adnan, S., Khan, A.H., 2009. Effective rainfall for irrigated agriculture plains of Pakistan. Pak. J. Meteorol. 6 (11), 61–72.

Ahmad, M.-u.-D., Bastiaanssen, W.M., Feddes, R., 2005. A new technique to estimate net groundwater use across large irrigated areas by combining remote sensing and water balance approaches, Rechna Doab, Pakistan. Hydrol. J. 13 (5), 653–664.

Ahmad, M.-u.-D., Turral, H., Nazeer, A., 2009. Diagnosing irrigation performance and water productivity through satellite remote sensing and secondary data in a large irrigation system of Pakistan. Agric. Water Manage. 96 (4), 551–564.

Ahmad, M.-u.-D., Masih, I., Giordano, M., 2014. Constraints and opportunities for water savings and increasing productivity through resource conservation technologies in Pakistan. Agric. Ecosyst. Environ. 187, 106–115.

Allen et al., 1998. Allen, R.G., Pereira, L.S., Raes, D., Smith, M., 1998. Crop Evapotranspiration-Guidelines for computing crop water requirements-FAO Irrigation and Drainage Paper No. 56. FAO, Rome 300, 6541.

Anuraga, T., Ruiz, L., Kumar, M.M., Sekhar, M., Leijnse, A., 2006. Estimating groundwater recharge using land use and soil data: a case study in South India. Agric. Water Manage. 84 (1), 65–76.

Awan, U.K., Ismaeel, A., 2014. A new technique to map groundwater recharge in irrigated areas using a SWAT model under changing climate. J. Hydrol. 519, 1368–1382.

Awan, U., Tischbein, B., Martius, C., 2013. Combining hydrological modeling and GIS approaches to determine the spatial distribution of groundwater recharge in an arid irrigation scheme. Irrig. Sci. 31 (4), 793–806.

Awan, U.K., Anwar, A., Ahmad, W., Hafeez, M., 2016. A methodology to estimate equity of canal water and groundwater use at different spatial and temporal scales: a geo-informatics approach. Environ. Earth Sci. 75 (5), 1–13.

Becker, M.W., 2006. Potential for satellite remote sensing of ground water. Groundwater 44 (2), 306–318.

Bhatti, A.M., Suttinon, P., Nasu, S., 2009. Agriculture water demand management in Pakistan: a review and perspective. Soc. Soc. Manag. Syst. 9 (172), 1–7.

Boegh, E., Poulsen, R.N., Butts, M., Abrahamsen, P., Dellwik, E., Hansen, S., Hasager, C.B., Ibrom, A., Loerup, J.K., Pilegaard, K., Soegaard, H., 2009. Remote sensing based evapotranspiration and runoff modeling of agricultural, forest and urban flux sites in Denmark: from field to macro-scale. J. Hydrol. 377 (3–4), 300–316.

Brunner, P., Hendricks Franssen, H.J., Kgotlhang, L., Bauer-Gottwein, P., Kinzelbach, W., 2007. How can remote sensing contribute in groundwater modeling?. Hydrol. J. 15 (1), 5–18.

Brutsaert, W., Stricker, H., 1979. An advection-aridity approach to estimate actual regional evapotranspiration. Water Resour. Res. 15 (2), 443–450.

Byun, K., Liaqat, U.W., Choi, M., 2014. Dual-model approaches for evapotranspiration analyses over homo-and heterogeneous land surface conditions. Agric. Forest Meteorol. 197, 169–187.

Campos, I., Villodre, J., Carrara, A., Calera, A., 2013. Remote sensing-based soil water balance to estimate Mediterranean holm oak savanna (dehesa) evapotranspiration under water stress conditions. J. Hydrol. 494, 1–9.

Castaño, S., Sanz, D., Gómez-Alday, J.J., 2010. Methodology for quantifying groundwater abstractions for agriculture via remote sensing and GIS. Water Resour. Manage. 24 (4), 795–814.

Cheema, M., Immerzeel, W., Bastiaanssen, W., 2014. Spatial quantification of groundwater abstraction in the Irrigated Indus Basin. Groundwater 52 (1), 25–36.

Choi, M., Kustas, W.P., Anderson, M.C., Allen, R.G., Li, F., Kjaersgaard, J.H., 2009. An intercomparison of three remote sensing-based surface energy balance algorithms over a corn and soybean production region (Iowa, US) during SMACEX. Agric. Forest Meteorol. 149 (12), 2082–2097.

Choi, M., Kim, T.W., Park, M., Kim, S.J., 2011. Evapotranspiration estimation using the Landsat-5 thematic mapper image over the Gyungan watershed in Korea. Int. J. Remote Sens. 32 (15), 4327–4341.

Chowdary, V.M., Chandran, R.V., Neeti, N., Bothale, R.V., Srivastava, Y.K., Ingle, P., Ramakrishnan, D., Dutta, D., Jeyaram, A., Sharma, J.R., Singh, R., 2008. Assessment of surface and sub-surface waterlogged areas in irrigation command areas of Bihar state using remote sensing and GIS. Agric. Water Manage. 95 (7), 754–766.

Cragoa, R., Brutsaert, W., 1996. Daytime evaporation and the self-preservation of the evaporative fraction and the bowen ratio. J. Hydrol. 178 (1), 241–255.

Crosbie, R., Davies, P., Harrington, N., Lamontagne, S., 2015. Ground truthing groundwater-recharge estimates derived from remotely sensed evapotranspiration: a case in South Australia. Hydrol. J. 23 (2), 335–350.

De Vries, J.J., Simmers, I., 2002. Groundwater recharge: an overview of processes and challenges. Hydrol. J. 10 (1), 5–17.

Ershadi, A., McCabe, M.F., Evans, J.P., Mariethoz, G., Kavetski, D., 2013. A Bayesian analysis of sensible heat flux estimation: quantifying uncertainty in meteorological forcing to improve model prediction. Water Resour. Res. 49 (5), 2343–2358.

Ershadi, A., McCabe, M.F., Evans, J.P., Walker, J.P., 2013. Effects of spatial aggregation on the multi-scale estimation of evapotranspiration. Remote Sens. Environ. 131, 51–62.

Ershadi, A., McCabe, M.F., Evans, J.P., Chaney, N.W., Wood, E.F., 2014. Multi-site evaluation of terrestrial evaporation models using FLUXNET data. Agric. Forest Meteorol. 187, 46–61.

Gibson, L., Münch, Z., Engelbrecht, J., 2011. Particular uncertainties encountered in using a pre-packaged SEBS model to derive evapotranspiration in a heterogeneous study area in South Africa. Hydrol. Earth Syst. Sci. 15 (1), 295–310.

Gowda, P.H., Howell, T.A., Paul, G., Colaizzi, P.D., Marek, T.H., Su, B., Copeland, K.S., 2013. Deriving hourly evapotranspiration rates with SEBS: a lysimetric evaluation. Vadose Zone J. 12 (3).

Hertzog, T., Poussin, J.-C., Tangara, B., Kouriba, I., Jamin, J.-Y., 2014. A role playing game to address future water management issues in a large irrigated system: experience from Mali. Agric. Water Manage. 137, 1–14.

Huang, C.-C., Yeh, H.-F., Lin, H.-I., Lee, S.-T., Hsu, K.-C., Lee, C.-H., 2013. Groundwater recharge and exploitative potential zone mapping using GIS and GOD techniques. Environ. Earth Sci. 68 (1), 267–280.

Hussain, I., Hussain, Z., Sial, M.H., Akram, W., Farhan, M., 2011. Water balance, supply and demand and irrigation efficiency of Indus Basin. Pak. Econ. Soc. Rev. 13–38.

Kinzelbach, W., Bauer, P., Siegfried, T., Brunner, P., 2003. Sustainable groundwater management–problems and scientific tool. Episodes 26 (4), 279–284.

Kirby, J.M., Ahmad, M.D., Mainuddin, M., Palash, W., Quadir, M.E., Shah-Newaz, S.M., Hossain, M.M., 2015. The impact of irrigation development on regional groundwater resources in Bangladesh. Agric. Water Manage. 159, 264–276.

Kirby, M., Ahmad, M.-u.-D., Mainuddin, M., Khaliq, T., Cheema, M.J.M., 2016. Agricultural production, water use and food availability in Pakistan: historical trends, and projections to 2050. Agric. Water Manage. http://dx.doi.org/10.1016/j.agwat.2016.06.001.

Laghari, A., Vanham, D., Rauch, W., 2012. The Indus basin in the framework of current and future water resources management. Hydrol. Earth Syst. Sci. 16, 1063–1083.

Liaqat, U.W., Choi, M., 2015. Surface energy fluxes in the Northeast Asia ecosystem: SEBS and METRIC models using Landsat satellite images. Agric. Forest Meteorol. 214–215, 60–79.

Liaqat, U.W., Choi, M., Awan, U.K., 2015. Spatio-temporal distribution of actual evapotranspiration in the Indus Basin irrigation system. Hydrol. Processes 29 (11), 2613–2627.

Liou, Y.-A., Kar, S.K., 2014. Evapotranspiration estimation with remote sensing and various surface energy balance algorithms—a review. Energies 7 (5), 2821–2849.

Liu, S., Sun, R., Sun, Z., Li, X., Liu, C., 2006. Evaluation of three complementary relationship approaches for evapotranspiration over the Yellow River basin. Hydrol. Processes 20 (11), 2347–2361.

Műnch, Z., Conrad, J.E., Gibson, L.A., Palmer, A.R., Hughes, D., 2013. Satellite earth observation as a tool to conceptualize hydrogeological fluxes in the Sandveld, South Africa. Hydrol. J. 21 (5), 1053–1070.

Mastrocicco, M., Colombani, N., Salemi, E., Castaldelli, G., 2010. Numerical assessment of effective evapotranspiration from maize plots to estimate groundwater recharge in lowlands. Agric. Water Manage. 97 (9), 1389–1398.

McCabe, M.F., Kalma, J.D., Franks, S.W., 2005. Spatial and temporal patterns of land surface fluxes from remotely sensed surface temperatures within an uncertainty modelling framework. Hydrol. Earth Syst. Sci. 9 (5), 467–480.

Milewski, A., Sultan, M., Yan, E., Becker, R., Abdeldayem, A., Soliman, F., Gelil, K.A., 2009. A remote sensing solution for estimating runoff and recharge in arid environments. J. Hydrol. 373 (1–2), 1–14.

Priestley, C., Taylor, R., 1972. On the assessment of surface heat flux and evaporation using large-scale parameters. Monthly Weather Rev. 100 (2), 81–92.

Santos, C., Lorite, I., Tasumi, M., Allen, R., Fereres, E., 2008. Integrating satellite-based evapotranspiration with simulation models for irrigation management at the scheme level. Irrig. Sci. 26 (3), 277–288.

Sarwar, A., Eggers, H., 2006. Development of a conjunctive use model to evaluate alternative management options for surface and groundwater resources. Hydrol. J. 14 (8), 1676–1687.

Scanlon, B.R., Healy, R.W., Cook, P.G., 2002. Choosing appropriate techniques for quantifying groundwater recharge. Hydrol. J. 10 (1), 18–39.

Scott, C.A., Shah, T., 2004. Groundwater overdraft reduction through agricultural energy policy: insights from India and Mexico. Int. J. Water Resour. Dev. 20 (2), 149–164.

Shafeeque, M., Cheema, M.J.M., Sarwar, A., Hussain, M.W., 2016. Quantification of groundwater abstraction using SWAT model in Hakra branch canal system of Pakistan. Pak. J. Agric. Sci. 53 (1), 249–255.

Singh, R.K., Irmak, A., 2011. Treatment of anchor pixels in the METRIC model for improved estimation of sensible and latent heat fluxes. Hydrol. Sci. J. 56 (5), 895–906.

Su, H., McCabe, M., Wood, E., Su, Z., Prueger, J., 2005. Modeling evapotranspiration during SMACEX: Comparing two approaches for local-and regional-scale prediction. J. Hydrometeorol. 6 (6), 910–922.

Su, Z., 2002. The surface energy balance system (SEBS) for estimation of turbulent heat fluxes. Hydrol. Earth Syst. Sci. 6 (1), 85–99.

Sugita, M., Brutsaert, W., 1991. Daily evaporation over a region from lower boundary layer profiles measured with radiosondes. Water Resour. Res. 27 (5), 747–752.

Szilágyi, J., Kovács, , Józsa, J., 2012. Remote-sensing based groundwater recharge estimates in the danube-tisza sand plateau region of Hungary. J. Hydrol. Hydromech. 60 (1), 64–72.

Szilagyi, J., Jozsa, J., 2013. MODIS-Aided statewide net groundwater-recharge estimation in nebraska. Groundwater 51 (5), 735–744.

Szilagyi et al., 2011. J. Szilagyi, V.A. Zlotnik, J.B. Gates, J. Jozsa, Mapping mean annual groundwater recharge in the Nebraska Sand Hills, USA, Hydrol. J. 19 (8) (2011) 1503–1513.

Ullah, M.K., Habib, Z., Muhammad, S., 2001. Spatial distribution of reference and potential evapotranspiration across the Indus Basin Irrigation Systems, Pakistan country series no.8, Working paper 24. IWMI, Lahore, Pakistan, p. 55.

Yang, X., Chen, Y., Pacenka, S., Gao, W., Zhang, M., Sui, P., Steenhuis, T.S., 2015. Recharge and groundwater use in the north China plain for six irrigated crops for an eleven year period. PLoS One 10 (1), e0115269.

Yu, W., Yang, Y.-C., Savitsky, A., Alford, D., Brown, C., Wescoat, J., Debowicz, D., Robinson, S., 2013. The Indus Basin of Pakistan: The Impacts of Climate Risks on Water and Agriculture. World Bank Publications.